





# Nonlocal exchange and correlation energy functionals using the Yukawa potential as ingredient: Application to the linear response of the uniform electron gas

Lucian A. Constantin <sup>1</sup>, Fulvio Sarcinella <sup>2,3</sup>, Eduardo Fabiano <sup>2,4</sup> and Fabio Della Sala <sup>2,4</sup>

<sup>1</sup>*Istituto di Nanoscienze, Consiglio Nazionale delle Ricerche (CNR-NANO), 41125 Modena, Italy*

<sup>2</sup>*Center for Biomolecular Nanotechnologies, Istituto Italiano di Tecnologia, Via Barsanti 14, 73010 Arnesano (LE), Italy*

<sup>3</sup>*Department of Mathematics and Physics “E. De Giorgi”, University of Salento, Via Arnesano, Lecce, Italy*

<sup>4</sup>*Institute for Microelectronics and Microsystems (CNR-IMM), Via Monteroni, Campus Unisalento, 73100 Lecce, Italy*



(Received 21 July 2021; accepted 21 September 2021; published 7 October 2021)

We show that the reduced, dimensionless Yukawa potential  $y_\alpha$  can be employed as an important ingredient in the construction of the exchange and correlation energy functionals. A functional based on  $y_\alpha$  provides a better description of the exchange and correlation linear response functions of the homogeneous electron gas, not only at small wave vectors, where gradient expansions are correct, but also at large wave vectors, where semilocal exchange and correlation functionals fail badly. Moreover, the  $y_\alpha$  ingredient gives a realistic description of the exchange energy and potential at the nuclear cusp and the inner atomic core, where the semilocal ingredients (i.e., the reduced gradient and Laplacian of the density) are not suitable, causing divergence of the potential. Thus, the  $y_\alpha$  ingredient can be attractive for the development of various exchange-correlation functionals.

DOI: [10.1103/PhysRevB.104.165114](https://doi.org/10.1103/PhysRevB.104.165114)

## I. INTRODUCTION

The Kohn-Sham (KS) density functional theory (DFT) [1–6] is the most used electronic structure computational method in quantum chemistry and solid-state physics [7]. In KS-DFT, the noninteracting kinetic energy is treated exactly using the KS one-particle orbitals, and only the exchange-correlation (XC) energy  $E_{xc}[n]$  must be approximated as a functional of the electronic density  $n(\mathbf{r})$ . The exact XC functional contains all the many-body quantum effects beyond the Hartree approximation, and due to its complexity, it is known only for few and very simple real systems, e.g., the dissociation of the  $H_2$  molecule [8]. Moreover, even the evaluation of the *almost*-exact XC potentials [ $v_{xc}(\mathbf{r}) = \delta E_{xc}[n(\mathbf{r})]/\delta n(\mathbf{r})$ ] from correlated *ab initio* densities requires nontrivial techniques, such as the inverse DFT problem of mapping the ground state density into its XC potential [9]. Despite these difficulties, the XC functional development has been an active research field for several decades [2–7, 10–13]. Nowadays many XC functionals have been developed [10–12, 14, 15], being accurate for various systems and properties.

The nonempirical XC functionals have been classified on the so-called DFT Jacob’s ladder [16], starting with the local (rung 1) and the generalized-gradient approximation (GGA, rung 2) semilocal ones. Meta-GGA functionals (rung 3) are the most sophisticated semilocal XC functionals, with the XC energy per particle [defined as  $E_{xc} = \int d\mathbf{r} n(\mathbf{r}) \epsilon_{xc}(\mathbf{r})$ ]

$$\epsilon_{xc}^{\text{semilocal}}(\mathbf{r}) = \epsilon_{xc}(n_\uparrow, n_\downarrow, \nabla n_\uparrow, \nabla n_\downarrow, \nabla^2 n_\uparrow, \nabla^2 n_\downarrow, \tau_\uparrow, \tau_\downarrow), \quad (1)$$

where  $n_\uparrow$ ,  $n_\downarrow$  are the spin densities ( $n = n_\uparrow + n_\downarrow$ ), and  $\tau_\uparrow$ ,  $\tau_\downarrow$  are the spin-dependent kinetic energy densities

( $\tau_\sigma = \sum_{i=1}^{\text{occ}} |\nabla \phi_{i,\sigma}|^2/2$ , where  $\phi_{i,\sigma}$  is the  $i$ th occupied KS orbital of spin  $\sigma$ ).

The semilocal ingredients, shown in Eq. (1), contain information only from an infinitesimal volume around  $\mathbf{r}$ , then the semilocal XC approximations cannot describe in detail many nonlocal features, even if they still may be accurate due to an error cancellation between the semilocal exchange and correlation functionals [17]. A simple way to develop nonlocal XC functionals is to use physically motivated orbital-free nonlocal ingredients, such as exchange-hole models [18–24], XC hole models [25–27], or the reduced Hartree potential [28, 29]

$$\eta^u = \frac{u(\mathbf{r})}{3(3/\pi)^{1/3} n(\mathbf{r})^{1/3}}, \quad (2)$$

where  $u(\mathbf{r}) = \int d\mathbf{r}' n(\mathbf{r}')/|\mathbf{r} - \mathbf{r}'|$  is the Hartree potential.

The reduced Hartree ingredient is important for one- and two-electron systems, but it is ill defined for extended systems. Recently, we have proposed the dimensionless, reduced Yukawa potential (also known as reduced screened Hartree potential) [30]

$$y_\alpha(\mathbf{r}) = \frac{\alpha^2}{4\pi n^{1/3}(\mathbf{r})} \int d\mathbf{r}' \frac{n(\mathbf{r}')}{|\mathbf{r} - \mathbf{r}'|} e^{-\alpha n^{1/3}(\mathbf{r})|\mathbf{r} - \mathbf{r}'|}, \quad (3)$$

which is of interest for the nonlocal kinetic energy functionals [30]. Here,  $\alpha \geq 0$  is a parameter that measures the screening strength. Semilocal functionals which include  $y_\alpha(\mathbf{r})$  as an ingredient have been named yGGA functionals [30].

Rung 4 of the ladder is represented by hybrid and hyper-GGA functionals [31–42], which use the nonlocal exact exchange as an ingredient. Finally, the most sophisticated XC functionals depend on all the occupied and unoccupied KS orbitals and energies (rung 5). They can be related to

the DFT perturbation theory [43–47], the interaction strength interpolation along the adiabatic connection curve [48–67], or the XC kernel approximations ( $f_{xc}$ ) for the linear-response time-dependent DFT approach, in the framework of the adiabatic-connection fluctuation-dissipation theorem [68–87].

All these XC approximations have been developed taking into account different exact conditions [88,89]. One of these is the XC linear response function of the homogeneous electron gas (HEG, also named jellium), defined as

$$\gamma_{xc}(\eta) = -\frac{k_F^2}{\pi} \mathcal{F} \left( \left. \frac{\delta^2 E_{xc}[n]}{\delta n(\mathbf{r}) \delta n(\mathbf{r}')} \right|_{n_0} \right) = \frac{f_{xc}(\eta)}{f_x^{\text{LDA}}}, \quad (4)$$

where  $\mathcal{F}$  represents the Fourier transform,  $\eta = k/(2k_F)$  is the dimensionless momentum [ $k_F = (3\pi^2 n_0)^{1/3}$  being the Fermi wave vector of the jellium model with the constant density  $n_0$ ],  $f_{xc}(\eta)$  is the HEG XC kernel, and  $f_x^{\text{LDA}} = -\pi/k_F^2$  is the LDA HEG exchange-only kernel. Accurate values of  $\gamma_{xc}(\eta)$  are known from quantum Monte Carlo calculations [90], being modeled in detail by several HEG XC kernel approximations, such as the state-of-the-art Richardson-Ashcroft (RA) jellium kernel [77]. Accurate description of the XC linear response function  $\gamma_{xc}(\eta)$  is a difficult requirement for many XC functionals of Jacob's ladder. In fact, the local density approximation (LDA) XC functional [1,91], which is constructed from the HEG, is exact for the jellium XC energy per particle ( $\epsilon_{xc}$ ), but its linear response  $\gamma_{xc}^{\text{LDA}}(\eta)$  is exact only at  $\eta = 0$ , being just a constant [ $\gamma_{xc}^{\text{LDA}}(\eta) = \gamma_{xc}^{\text{LDA}}(0)$ ]. On the other hand, the exchange and correlation gradient expansions [92–97] are exact in the limit  $\eta \rightarrow 0$ , while they fail abruptly at large wave vectors, where they diverge [98]. For this reason, several generalized gradient approximations (GGAs) [99–101], meta-GGAs [15,88], global hybrids [42], and long-range [102] and short-range screened hybrids [103,104] have been constructed to recover the LDA linear response.

The violation of the correct  $\eta \rightarrow \infty$  behavior of the XC kernel can also cause the so-called ultraviolet catastrophe which produces a divergence of the pair distribution function at small interparticle distances [81,105].

In this article, we study the significance of the reduced Yukawa potential  $y_\alpha(\mathbf{r})$  [see Eq. (3)] for exchange and correlation functionals, showing its relevance for the XC HEG linear response function  $\gamma_{xc}(\eta)$ .

The paper is organized as follows. In Sec. II and Sec. III, we propose very simple exchange and correlation functionals using the reduced Yukawa potential as the only ingredient, and show results for atoms and jellium clusters. In Sec. IV, we combine the exchange and correlation functionals of the previous sections, to show results for the full XC functional. Finally, conclusions are drawn in Sec. V.

## II. EXCHANGE ENERGY FUNCTIONALS

### A. Development of the exchange functionals

First, let us consider the most simple,  $y_\alpha(\mathbf{r})$ -dependent exchange functional, which we name YUKx0, whose enhancement factor  $F_x$  (defined as  $\epsilon_x = \epsilon_x^{\text{LDA}} F_x$ ) is

$$F_x^{\text{YUKx0}} = y_\alpha. \quad (5)$$

For any value of the  $\alpha \geq 0$  parameter, YUKx0 recovers the LDA for the HEG, and behaves correctly under the uniform density scaling of the density ( $E_x^{\text{YUKx0}}[n_\lambda] = \lambda E_x^{\text{YUKx0}}[n]$ , where  $n_\lambda(\mathbf{r}) = \lambda^3 n(\lambda \mathbf{r})$ , with  $\lambda \geq 0$ ). Performing similar calculations to those in Ref. [30], see also Appendix B, we obtain the following HEG linear response function:

$$\gamma_x^{\text{YUKx0}}(\eta) = \frac{\alpha^4 + 14\alpha_{k_F}^2 \alpha^2 \eta^2 - 8\alpha_{k_F}^4 \eta^4}{(4\alpha_{k_F}^2 \eta^2 + \alpha^2)^2}, \quad (6)$$

where  $\alpha_{k_F} = (3\pi^2)^{(1/3)}$ . When  $\eta \rightarrow 0$  it behaves as

$$\gamma_x^{\text{YUKx0}} \rightarrow 1 + 6 \frac{\alpha_{k_F}^2}{\alpha^2} \eta^2 - 72 \frac{\alpha_{k_F}^4}{\alpha^4} \eta^4 + O(\eta^6), \quad (7)$$

and we recall that the exact response function [92] gives  $\gamma_x^{\text{exact}} \rightarrow 1 + (5/9)\eta^2 + (73/225)\eta^4 + O(\eta^6)$ ; see also Appendix B. Then, we require that YUKx0 recover the second-order term at small wave vectors, and we obtain

$$\alpha = \frac{3}{5} \sqrt{30} \alpha_{k_F}. \quad (8)$$

This condition is also fulfilled by any semilocal exchange functional that recovers the second-order gradient expansion (GE2) of the exchange energy (i.e.,  $\epsilon_x^{\text{GE2}} = \epsilon_x^{\text{LDA}}(1 + \mu_x s^2)$ , where  $\mu_x = 10/81$  [93] and  $s = |\nabla n|/(2k_F n)$  being the reduced gradient of the density). For example, the popular PBEsol GGA [106] behaves as GE2, yielding  $\gamma_x^{\text{PBEsol}} = \gamma_x^{\text{GE2}} = 1 + (9/2)\mu_x \eta^2$ , being accurate at small wave vectors, but diverging at large wave vectors, where the exact response function vanishes as [ $\gamma_x^{\text{exact}} \rightarrow 1/(2\eta^2)$ ]. (A complete analysis of the HEG linear response of semilocal exchange functionals is presented in Appendix B.) On the other hand, the YUKx0 is finite when  $\eta \rightarrow \infty$ , but has the wrong sign, behaving as

$$\gamma_x^{\text{YUKx0}} \rightarrow -\frac{1}{2} + \frac{9}{8} \frac{\alpha^2}{\alpha_{k_F}^2 \eta^2} - \frac{15}{32} \frac{\alpha^4}{\alpha_{k_F}^4 \eta^4} + O(\eta^{-6}). \quad (9)$$

In order to solve this problem, we next propose the YUKx1 exchange functional, with the following exchange enhancement factor,

$$F_x^{\text{YUKx1}} = (1 - \beta) + \beta y_\alpha, \quad (10)$$

where the parameters  $\beta$  and  $\alpha$  are fixed from the conditions (i)  $\gamma_x^{\text{YUKx1}} \rightarrow 1 + (5/9)\eta^2 + \dots$  at small  $\eta$ , and (ii)  $\gamma_x^{\text{YUKx1}} \rightarrow 0$  at large  $\eta$ . We obtain the following parameters:

$$\begin{aligned} \alpha &= 6/5 \sqrt{5} \alpha_{k_F}, \\ \beta &= 2/3. \end{aligned} \quad (11)$$

With this choice of parameters, the YUKx1 exchange response function has the simple analytic expression (see Appendix B)

$$\gamma_x^{\text{YUKx1}} = 27 \frac{5\eta^2 + 3}{(5\eta^2 + 9)^2}, \quad (12)$$

which behaves as

$$\begin{aligned} \gamma_x^{\text{YUKx1}} &\rightarrow 1 + \frac{5}{9}\eta^2 - \frac{25}{27}\eta^4 + O(\eta^6), \text{ when } \eta \rightarrow 0, \\ \gamma_x^{\text{YUKx1}} &\rightarrow \frac{27}{5\eta^2} - \frac{81}{5\eta^4} + O(\eta^{-6}), \text{ when } \eta \rightarrow \infty. \end{aligned} \quad (13)$$

Note that YUKx0 and YUKx1 do not depend on the gradient of the density at all; thus they belong to the yLDA class of XC functionals. In this work, we will not consider functionals that depend also on the gradient, which will be investigated elsewhere. Note that the yLDA functionals investigated here do not include any empirical parameter.

Finally, we consider the YUKx2 exchange functional of the form

$$F_x^{\text{YUKx2}} = [1 - c(z)]\zeta_2 + c(z)F_x^{\text{YUKx1}}, \quad (14)$$

where

$$\zeta_2(\mathbf{r}) = \frac{1}{4An^{1/3}(\mathbf{r})} \int d\mathbf{r}' \frac{n(\mathbf{r}')}{|\mathbf{r} - \mathbf{r}'|} e^{-\alpha_2 c(z)n^{1/3}(\mathbf{r})|\mathbf{r} - \mathbf{r}'|}, \quad (15)$$

with  $A = 3\alpha_{k_F}/(4\pi)$ ,

$$c(z) = (1 - z^3)^{1/6}, \quad (16)$$

and  $z = \tau^W/\tau$  being the well-known meta-GGA ingredient. Here  $\tau^W = |\nabla n|^2/(8n)$  is the von Weizsäcker kinetic energy density. Note that the function  $c(z)$  has been previously used in Ref. [28]. The ingredient  $\zeta_2(\mathbf{r})$  is similar to  $y_\alpha(\mathbf{r})$ , but in the case of one- and two-electron systems, where  $c(z) = 0$ , it simplifies to Eq. (2).

Finally, the parameter  $\alpha_2$  has been fitted to the exchange energy of noble atoms (see Appendix C), being

$$\alpha_2 = 0.3\alpha_{k_F}. \quad (17)$$

The YUKx2 exchange functional is exact for any one- and two-electron systems, where

$$E_x[n] = -\frac{1}{2} \int d\mathbf{r} n(\mathbf{r}) u(\mathbf{r}), \quad \text{for } N = 1, \\ E_x[n] = -\frac{1}{4} \int d\mathbf{r} n(\mathbf{r}) u(\mathbf{r}), \quad \text{for } N = 2, \quad (18)$$

with  $u(\mathbf{r})$  being the Hartree potential and  $N$  the number of electrons. Moreover, YUKx2 preserves the HEG linear response of the YUKx1 functional (see Appendix C). Note, however, that the YUKx2 functional is not a yGGA functional as defined in Ref. [30], because it depends on the kinetic energy density and thus on KS orbitals.

## B. Results for exchange functionals

### 1. HEG linear response of the exchange energy

In Fig. 1, we show the HEG exchange-only linear-response (LR) function  $\gamma_x(\eta)$  of several exchange energy functionals. The LDA (with  $\gamma_x^{\text{LDA}} = 1$ ) is exact only at  $\eta = 0$ . On the other hand, PBE and PBEsol exchange functionals [with  $\gamma_x^{\text{GGA}} = 1 + (9/2)\mu_x\eta^2$  where  $\mu_x^{\text{PBE}} = 0.21951$  and  $\mu_x^{\text{PBEsol}} = 10/81$ ] are accurate at small wave vectors  $\eta < 1$  but they fail badly for  $\eta > 1$ . We recall that the large-wave-vector regime is dominant when the external perturbation of the HEG has a small amplitude and a short-wavelength density wave. On the other hand, the most accurate exchange functional is YUKx1 (and YUKx2), which is exact in both small- and large-wave-vector limits. However, we observe that the YUKx functionals, as well as all semilocal exchange functionals, cannot capture the abrupt behavior at  $\eta \rightarrow 1$ , where  $d\gamma_x^{\text{exact}}/d\eta \rightarrow -\infty$ .

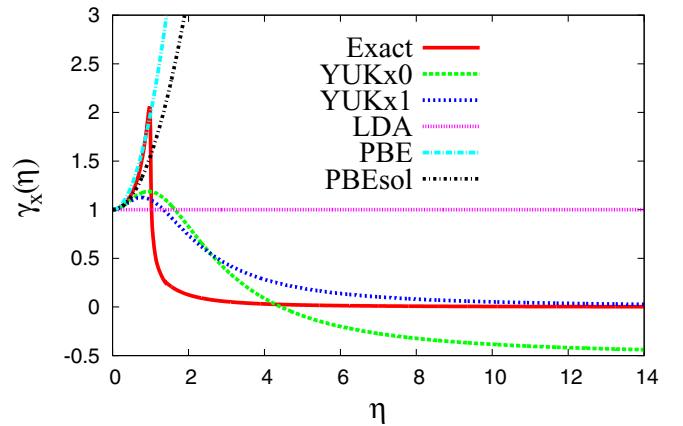


FIG. 1. The exchange-only LR function  $\gamma_x$  of the uniform electron gas, versus  $\eta = k/2k_F$ . Note that YUKx2 is the same as YUKx1.

### 2. Atoms

At the nuclear cusp and the inner atomic core, the exact exchange enhancement factor  $F_x^{\text{EXX}} = \epsilon_x^{\text{EXX,conv}}/\epsilon_x^{\text{LDA}}$ , defined in the conventional gauge [31,107] of the exact exchange energy per particle  $\epsilon_x^{\text{EXX,conv}}$ , has a significant de-enhancement (i.e.,  $F_x^{\text{EXX}} < 1$ ) that cannot be described by popular semilocal functionals, where  $F_x^{\text{semilocal}} \geq 1$ . In order to mimic the exact behavior, the Laplacian of the density  $\nabla^2 n$  must be involved in the functional expression [108], but it gives unphysical oscillations in the exchange potential ( $v_x = \delta E_x/\delta n$ ). Below we show that our simple but nonlocal exchange functionals can describe considerably better this atomic region. Next, we report in Fig. 2 the exchange enhancement factors for He, Ne, and Ar atoms see Appendix A for details. In the case of the He atom, the YUKx2 functional is exact by construction. YUKx0 and YUKx1 are unexpectedly accurate at the nucleus, showing a significant de-enhancement and being close to the exact value, as reported in Table I. On the other hand, the YUKx0 and YUKx1 functionals give relative errors of the He exchange energy of  $-6.9\%$  and  $-10.4\%$ , respectively, being better than LDA ( $-13.6\%$ ) but definitely worse than TPSS ( $0.6\%$ ); see Table I.

In the cases of Ne and Ar atoms, shown in the other panels of Fig. 2, all YUKx functionals have similar shapes of the exchange enhancement factor, modeling quite well the exact behavior at the nucleus and the inner atomic core, while uMGGA and TPSS are enhanced over the LDA everywhere in space. At the nuclear cusp, all YUKx are quite accurate, in contrast to LDA, TPSS, uMGGA, and SCAN; see also Table I. Regarding the total exchange energy, similar trends to those for helium are found.

To test in more detail the accuracy of these exchange functionals for atoms, we report in Fig. 3 the relative errors of exchange energy  $E_x$  (in %) of neutral, nonrelativistic noble, alkali, and alkali-earth atoms, versus  $Z^{-1/3}$ , where  $Z$  is the nuclear charge ( $10 \leq Z \leq 292$ ). The limit  $Z \rightarrow \infty$  represents the semiclassical atom that is described by the semiclassical asymptotic expansion [109–111]

$$E_x[n] \approx E_x^{\text{LDA}} + d_1 Z + d_2 Z^{2/3} + \dots, \quad (19)$$

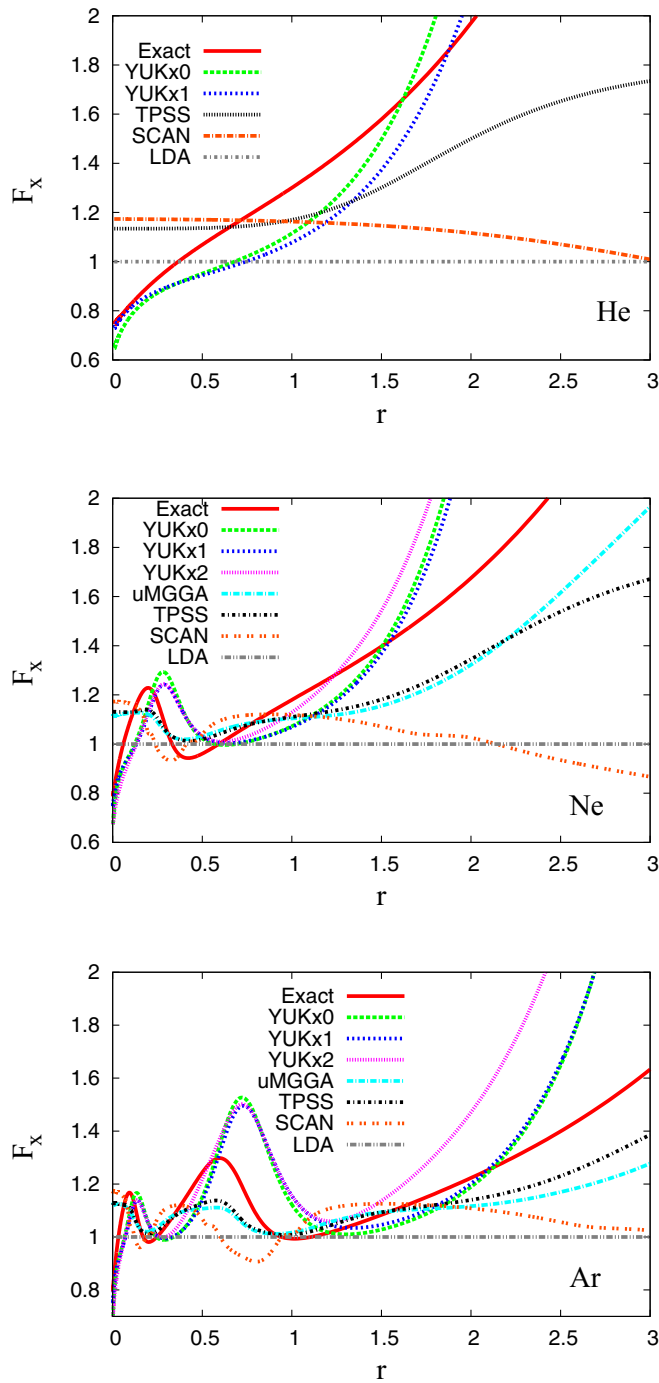


FIG. 2. Exchange enhancement factor  $F_x$  versus the radial distance from the nucleus  $r$  (in a.u.), for He atom (upper panel), Ne atom (middle panel), and Ar atom (lower panel). Note that YUKx2 and uMGGA are exact for He atom.

where  $d_1 = -0.2240$  and  $d_2 = 0.2467$  are atomic inner core and atomic quantum oscillation dependent terms, respectively. The most accurate functional is uMGGA [28], which has been constructed to recover Eq. (19). Nevertheless, the YUKx functionals become accurate for large atoms, with errors below 1%, and competing with the TPSS meta-GGA. This is an important achievement of the YUKx0 and YUKx1 functionals,

TABLE I. Exchange enhancement factor  $F_x(0)$  at the nuclear cusp, relative error in the total exchange energy ( $\Delta E_x$ ), and the exchange potential  $v_x(0)$  at the nuclear cusp. N.C. means that the exchange potential can only be defined using an optimized effective potential procedure, not considered in this work.

	$F_x(0)$	$\Delta E_x$	$v_x(0)$
He			
exact	0.75	0	-1.65
YUKx0	0.65	-6.93%	-1.52
YUKx1	0.73	-10.39%	-1.49
YUKx2	0.75	0	-1.65
umGGA	0.75	0	-1.65
LDA	1	-13.65%	-1.48
PBE	1	-0.84%	$-\infty$
TPSS	1.13	0.63%	
SCAN	1.17	0.67%	
Ne			
exact	0.79	0	-7.94
YUKx0	0.67	-1.75%	-8.47
YUKx1	0.75	-3.15%	-8.41
YUKx2	0.68	-2.41%	N.C.
umGGA	1.11	0.47%	$-\infty$
LDA	1	-8.67%	-8.27
PBE	1.03	-0.12%	$-\infty$
TPSS	1.13	0.79%	$-\infty$
SCAN	1.17	0.60%	$-\infty$
Ar			
exact	0.79	0	-14.33
YUKx0	0.68	-2.01%	-15.45
YUKx1	0.75	-2.57%	-15.39
YUKx2	0.69	-0.88%	N.C.
umGGA	1.12	0.09%	$-\infty$
LDA	1	-7.58%	-15.21
PBE	1.03	-0.53%	$-\infty$
TPSS	1.13	0.19%	$-\infty$
SCAN	1.17	0.32%	$-\infty$

because they have been constructed solely from the HEG linear response. On the other hand, YUKx2, which performs better, has a parameter fitted to the noble atoms.

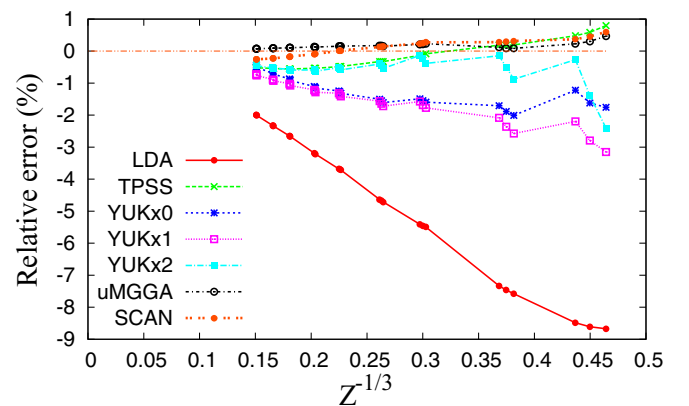


FIG. 3. Relative errors of exchange energy  $E_x$  (in %) for noble atoms for  $10 \leq Z \leq 290$ , alkali atoms for  $11 \leq Z \leq 291$ , and alkali-earth atoms for  $12 \leq Z \leq 292$ .

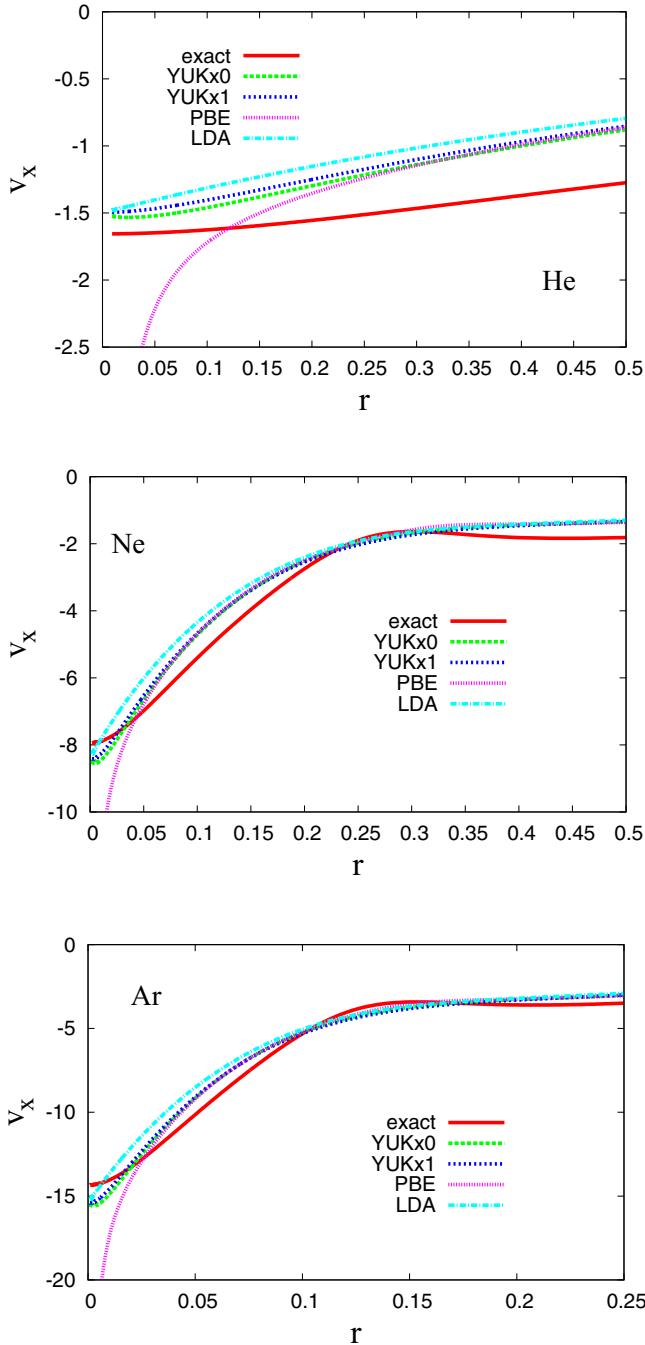


FIG. 4. The exchange potential  $v_x = \delta E_x / \delta n$  (in a.u.) versus the radial distance (in a.u.) from the nucleus  $r$ , for He, Ne, and Ar atoms.

### 3. Exchange potential for atoms

The good performance of the YUKx0 and YUKx1 exchange enhancement factors at the nuclear cusp needs to be confirmed considering the first functional derivative, i.e., the exchange potential.

The exchange potential for the yGGA functional has the following expression [30]:

$$v_x = v_x^{(0)} + v_x^{(1)} + v_x^{(2)},$$

$$v_x^{(0)} = \frac{\partial e_x}{\partial n} - \nabla \frac{\partial e_x}{\partial \nabla n} + \nabla^2 \frac{\partial e_x}{\partial \nabla^2 n},$$

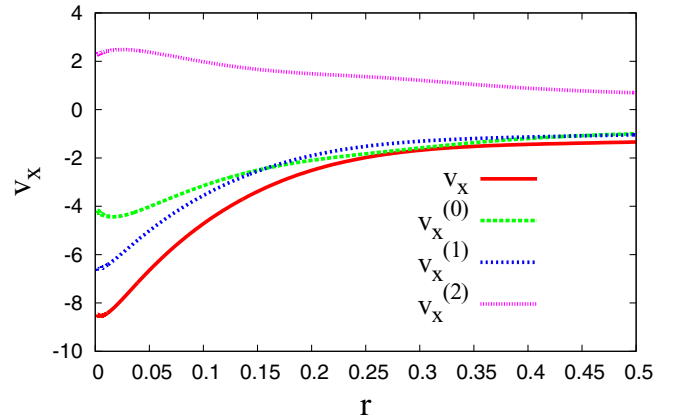


FIG. 5. The total exchange potential  $v_x$  (in a.u.), and its components ( $v_x^{(0)}$ ,  $v_x^{(1)}$ , and  $v_x^{(2)}$ ) of Eq. (20), in the case of YUKx0 functional and Ne atom, as a function of the radial distance (in a.u.).

$$v_x^{(1)} = \int d\mathbf{r}' \frac{\partial e_x}{\partial u_\alpha}(\mathbf{r}') \frac{e^{-\alpha n^{1/3}(\mathbf{r}')|\mathbf{r}-\mathbf{r}'|}}{|\mathbf{r}-\mathbf{r}'|},$$

$$v_x^{(2)} = -\frac{\alpha}{3n^{2/3}(\mathbf{r})} \frac{\partial e_x}{\partial u_\alpha}(\mathbf{r}) \int d\mathbf{r}' n(\mathbf{r}') e^{-\alpha n^{1/3}(\mathbf{r})|\mathbf{r}-\mathbf{r}'|}, \quad (20)$$

where  $u_\alpha = \int d\mathbf{r}' \frac{n(\mathbf{r}')}{|\mathbf{r}-\mathbf{r}'|} e^{-\alpha n^{1/3}(\mathbf{r}')|\mathbf{r}-\mathbf{r}'|}$  is the Yukawa screened potential (i.e.,  $u_\alpha(\mathbf{r}) = y_\alpha(\mathbf{r})[4\pi n^{1/3}(\mathbf{r})]/\alpha^2$ ).

Note that the YUKx2 functional depends also on the kinetic energy density and thus on KS orbitals, and thus Eqs. (20) are not valid in this case. Investigations of the YUKx2 exchange potential, which require special techniques [15], will be presented elsewhere.

In Fig. 4, we show the exchange potential  $v_x = \delta E_x / \delta n$  versus the radial distance from the nucleus  $r$ , for several noble atoms. We observe that for all the considered atoms (He, Ne, and Ar), YUKx0 and YUKx1 exchange potentials are finite and accurate at the nucleus, being close to the LDA, in contrast to semilocal functionals which diverge at the nucleus [ $v_x^{\text{semilocal}}(r \rightarrow 0) \rightarrow -\infty$ ]. Despite the YUKx potentials are close to LDA, the YUKx have better enhancement factors  $F_x$ ; see Table I. Values of the exchange potential at the nuclear cusp are reported in the last column of Table I: relative errors for YUKx functional are within 8% for all cases. Moreover, as shown in Fig. 5, all the components of  $v_x$  (i.e.,  $v_x^{(0)}$ ,  $v_x^{(1)}$ , and  $v_x^{(2)}$ ) are finite at the nucleus, and the main contribution is given by  $v_x^{(1)}$ .

### 4. Jellium clusters

Next, we consider neutral jellium clusters with  $Z$  electrons and radius  $R = r_s Z^{1/3}$ ; see Appendix A for details. Such jellium spheres are simple models for simple metal clusters, which are of interest in various applications [112,113]. In Table II, we report the error statistics (MARE and MAE) of exchange energy for jellium clusters with  $Z = 8, 18, 20, 34, 40, 58,$  and  $92$ , and bulk parameter  $r_s = 2$  and  $4$ , respectively. We observe that YUKx functionals improve considerably over LDA, being often comparable with TPSS and uMGGA. In particular YUKx0 is the most accurate between the yLDA functionals, while YUKx1 is the worst one, being closer to



TABLE II. Mean absolute relative errors (MARE in %) and mean absolute errors (MAE in a.u., shown in parentheses) of the exchange energy  $E_x$  for jellium clusters with  $Z = 8, 18, 20, 34, 40, 58$ , and  $92$ , and bulk parameter  $r_s = 2$  and  $r_s = 4$ , from various exchange functionals.

	$r_s = 2$	$r_s = 4$
LDA	4.03 (0.256)	4.13 (0.142)
PBE	0.68 (0.038)	0.59 (0.016)
TPSS	0.91 (0.058)	0.73 (0.024)
SCAN	0.18 (0.015)	0.51 (0.018)
uMGGA	0.86 (0.060)	0.76 (0.030)
YUKx0	0.87 (0.036)	1.40 (0.030)
YUKx1	1.83 (0.088)	2.56 (0.075)
YUKx2	1.09 (0.080)	1.31 (0.047)

LDA. In any case, such accuracy can be considered remarkable, taking into account that these YUKx functionals do not have any parameter fitted on jellium clusters or any gradient dependence.

We also tested jellium clusters with  $Z = 58$  and  $92 e^-$ , and  $2 \leq r_s \leq 6$  in a perturbed external potential of the following form:

$$v_{\text{ext}}(r) = v_{\text{ext}}^{\text{jell}}(r) \left[ 1 + \frac{1}{m} \sin(\kappa r) \right], \quad (21)$$

where  $v_{\text{ext}}^{\text{jell}}(r)$  is the external potential of the unperturbed jellium cluster; see Eq. (A1) of Appendix A. Similarly to the calculations of Ref. [30], we compute the exchange response of the functional  $E_x$ , as

$$\delta_{\kappa} E_x = (E_x[v_{\text{ext}}] - E_x[v_{\text{ext}}^{\text{jell}}]) / E_x[v_{\text{ext}}^{\text{jell}}] \times 100, \quad (22)$$

and we measure its  $\kappa$ -averaged exchange response error as

$$\Delta E_x = \int_{\kappa^{\text{min}}}^{\kappa^{\text{max}}} d\kappa |\delta_{\kappa} E_x - \delta_{\kappa} E_x^{\text{exact}}| / (\kappa^{\text{max}} - \kappa^{\text{min}}), \quad (23)$$

where  $\kappa^{\text{min}} = 0$ ,  $\kappa^{\text{max}} = 2.1$ , and  $m = 50$ . The results are shown in Table III, and we see that the LDA and YUKx functionals perform close to each other, and noticeably better than the PBE, TPSS, SCAN, and uMGGA functionals. In fact at high wave vectors, the LDA and YUKx HEG exchange response functions ( $\gamma_x$ ) remain finite, whereas for all the other functionals they diverge. Finally, we show in Fig. 6 the relative exchange response  $\delta_{\kappa} E_x$  [see Eq. (22)] versus  $\kappa$  of several exchange functionals, for the considered jellium clusters with  $r_s = 3$ . The exact exchange energy (EXX) oscillates with  $\kappa$ , and the frequency of these oscillations slightly increases from the  $Z = 58$  cluster to the one with  $Z = 92$ . All the functional approximations follow the EXX oscillations, having almost the same accuracy for  $\kappa \leq 0.75$ . However, for  $0.75 \leq \kappa \leq 2.1$ , YUKx0 performs better than SCAN and uMGGA, being significantly closer to EXX, especially for the cluster with  $Z = 92$ .

TABLE III. The  $\kappa$ -averaged exchange response errors [ $\Delta E_x$  of Eq. (23)] of various KE functionals, for the jellium clusters with 58 and  $92 e^-$ , in the case of several bulk parameters ( $2 \leq r_s \leq 6$ ). The last column shows the overall accuracy (averaged over  $r_s$ ). The best result of each column is highlighted in bold.

	$r_s = 2$	$r_s = 3$	$r_s = 4$	$r_s = 5$	$r_s = 6$	overall
Jellium cluster with 58 $e^-$						
LDA	0.60	<b>0.58</b>	<b>0.59</b>	<b>0.49</b>	<b>0.34</b>	<b>0.52</b>
PBE	0.50	0.89	1.20	1.27	1.27	1.03
TPSS	0.43	0.78	1.07	1.13	1.13	0.91
SCAN	0.45	0.84	1.08	1.02	1.01	0.89
uMGGA	0.50	0.89	1.20	1.27	1.25	1.02
YUKx0	0.53	0.61	0.64	0.55	0.41	0.55
YUKx1	0.62	0.63	0.63	0.53	0.39	0.56
YUKx2	<b>0.40</b>	<b>0.58</b>	0.69	0.67	0.59	0.59
Jellium cluster with 92 $e^-$						
LDA	0.46	<b>0.60</b>	<b>0.73</b>	0.73	0.63	0.63
PBE	0.78	1.49	2.08	2.23	2.14	1.74
TPSS	0.69	1.33	1.89	2.00	1.97	1.58
SCAN	1.01	1.53	1.90	1.80	1.84	1.62
uMGGA	0.80	1.46	1.99	2.11	2.02	1.68
YUKx0	<b>0.43</b>	0.69	0.83	0.78	0.59	0.67
YUKx1	0.48	0.63	0.74	<b>0.70</b>	<b>0.49</b>	<b>0.61</b>
YUKx2	0.56	0.95	1.31	1.30	1.26	1.08

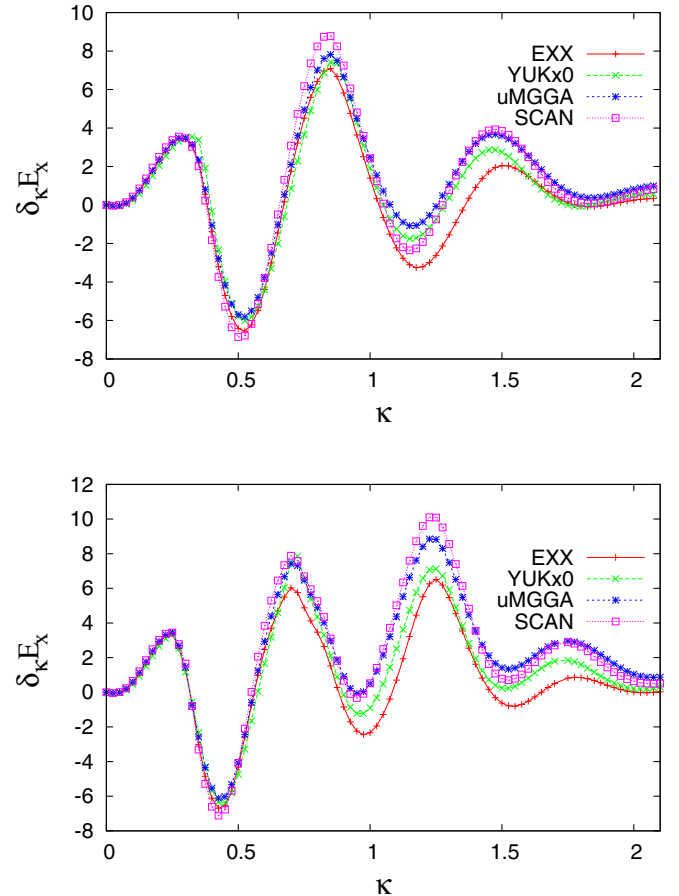


FIG. 6. Relative exchange response  $\delta_{\kappa} E_x$  [see Eq. (22)] versus  $\kappa$  (in a.u.) of several exchange functionals, for the jellium clusters with  $Z = 58$  (upper panel) and  $Z = 92$  (lower panel), and  $r_s = 3$ .

### III. CORRELATION FUNCTIONAL

We now move to analyze the HEG linear response of the correlation functional. The HEG linear response correlation function  $\gamma_c$  has the following properties:

(i) At small wave vectors, it behaves as [98]

$$\gamma_c(\eta) \rightarrow \gamma_c^{\text{LDA}} - \frac{3}{2}\beta(r_s)\pi^2\eta^2, \quad \text{when } \eta \rightarrow 0, \quad (24)$$

where a simple and accurate parametrization of the density-dependent GE2 correlation coefficient [94]  $\beta(r_s)$  has been proposed in Ref. [114],

$$\beta(r_s) \approx 0.066725 \frac{1 + 0.1r_s}{1 + 0.1778r_s}. \quad (25)$$

(ii) At large wave vectors, it behaves as [72,77]

$$\gamma_c(\eta) \rightarrow -\frac{2\pi}{k_F} \frac{d(r_s \epsilon_c^{\text{LDA}})}{dr_s}, \quad \text{when } \eta \rightarrow \infty. \quad (26)$$

For other wavevectors  $\gamma_c$  is very complicated, and it is better analyzed together with the exchange functional which is the topic of the next section.

Because the computation of the linear response correlation energy is very complicated, we construct the functional requiring the following features:

(a) at  $\eta = 0$  to recover  $\gamma_c^{\text{LDA}}$ , and at small wave vectors to obtain a negative slope ( $d\gamma_c/d\eta^2 \leq 0$ );

(b) at large wave vectors to model (as much as possible) the exact behavior of Eq. (26).

Moreover, in order to further simplify the calculations for the HEG linear response function of the correlation energy, we use the simple but accurate parametrization of the LDA correlation energy per particle proposed in Ref. [115],

$$\begin{aligned} \epsilon_c^{\text{LDA}}(r_s, \zeta) &= \epsilon_c^0(r_s) + [\epsilon_c^1(r_s) - \epsilon_c^0(r_s)]f(\zeta), \\ \epsilon_c^i &= -a_i \ln \left( 1 + \frac{b_i}{r_s} + \frac{b_i}{r_s^2} \right), \quad \text{with } i = 0, 1, \\ f(\zeta) &= [(1 + \zeta)^{4/3} + (1 - \zeta)^{4/3} - 2]/[2(2^{1/3} - 1)], \end{aligned} \quad (27)$$

where  $\zeta = (n_\uparrow - n_\downarrow)/n$  is the relative spin polarization, and  $\epsilon_c^0(r_s)$  and  $\epsilon_c^1(r_s)$  are the paramagnetic and the ferromagnetic correlation energies per particle, respectively, and the parameters are  $a_0 = (\ln 2 - 1)/(2\pi^2)$ ,  $b_0 = 20.4562557$ ,  $a_1 = (\ln 2 - 1)/(4\pi^2)$ , and  $b_1 = 27.4203609$ .

We find that the following correlation energy per particle satisfies the conditions (a) and (b):

$$\epsilon_c^{\text{YUKc}} = \epsilon_c^{\text{LDA}} \frac{1 + \sigma}{y_\alpha + \sigma}, \quad (28)$$

with  $\sigma=5$  and  $\alpha=2\alpha_{k_F}$ . (For some details, see Appendix D.) We remark that the YUKc correlation functional is not intended to be accurate for any system, with the exception of the HEG linear response regime. Nevertheless, the YUKc can be used as a starting point, for the construction of accurate nonlocal correlation functionals. In Fig. 7, we report  $\gamma_c^{\text{YUKc}}(\eta)$ , showing how it fulfills the conditions (a) and (b). Thus, YUKc recovers LDA at  $\eta = 0$ , and gives indeed negative slope  $d\gamma_c^{\text{YUKc}}(\eta)/d\eta^2 \leq 0$  when  $\eta \leq 0.5$ , such that for any bulk parameter  $r_s$ , it behaves at small wave

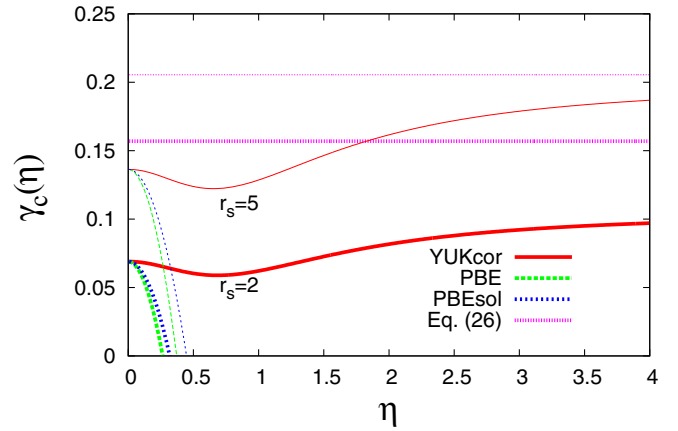


FIG. 7. The correlation-only HEG linear response function  $\gamma_c(\eta)$ , versus the dimensionless momentum  $\eta = k/2k_F$ , for  $r_s = 2$  (thick lines) and 5 (narrow lines), respectively. We also show the exact asymptote for large wave vectors [see Eq. (26)].

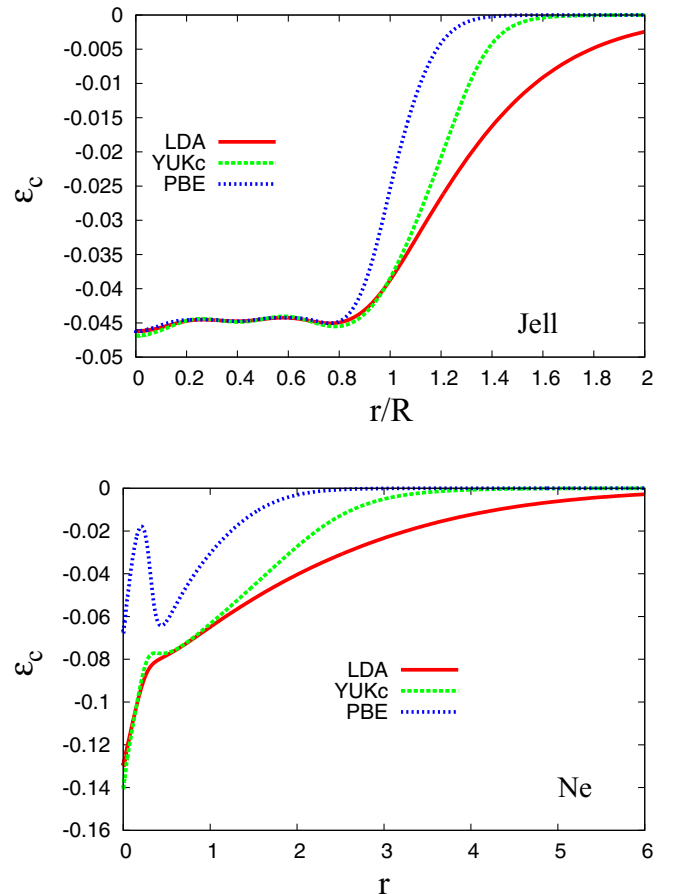


FIG. 8. Upper panel: Correlation energy per particle  $\epsilon_c$  (in a.u.) versus the scaled radial distance  $r/R$ , with  $R$  being the radius of the jellium cluster with 92  $e^-$ , and  $r_s = 2$ . The total correlation energies are (in a.u.)  $E_c^{\text{LDA}} = -3.9005$ ,  $E_c^{\text{YUKc}} = -3.8843$ , and  $E_c^{\text{PBE}} = -3.5195$ . Lower panel: Correlation energy per particle  $\epsilon_c$  versus the radial distance  $r$  (in a.u.) for the Ne atom. The total correlation energies are (in a.u.)  $E_c^{\text{LDA}} = -0.7428$ ,  $E_c^{\text{YUKc}} = -0.7188$ , and  $E_c^{\text{PBE}} = -0.3510$ .

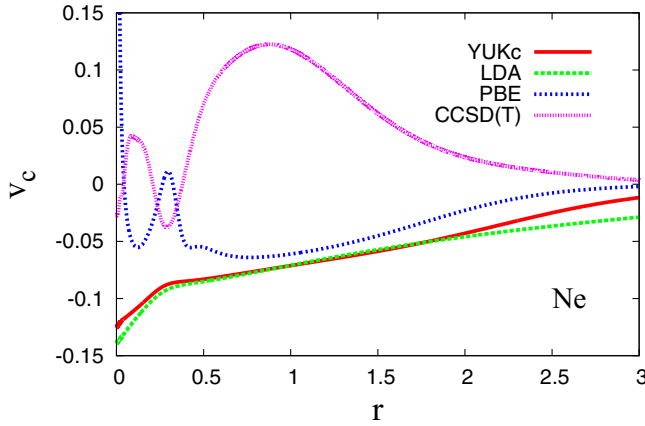


FIG. 9. The correlation potential  $v_c = \delta E_c / \delta n$  (in a.u.) versus the radial distance from the nucleus  $r$  (in a.u.), for Ne atom. The single, double, and partially triple excitations [CCSD(T)] reference curve is taken from Ref. [45].

vectors as  $\gamma_c^{\text{YUKc}} = \gamma_c^{\text{LDA}} - \frac{3}{2}\beta^{\text{YUKc}}(r_s)\pi^2\eta^2 + O(\eta^4)$ , where  $\beta^{\text{YUKc}}(2) \approx 0.005$  and  $\beta^{\text{YUKc}}(5) \approx 0.007$ , i.e. about one order of magnitude smaller than the exact GE2 parameter  $\beta(r_s)$  of Eq. (25). On the other hand, at large wave vectors,  $\gamma_c^{\text{YUKc}}(\eta)$  mimics the exact behavior of Eq. (26) which is a very difficult exact condition for correlation functionals. In fact, to our best knowledge, only the jellium XC kernels [72,75,77,80,86] used in the linear-response time-dependent DFT approach, in the context of the adiabatic connection fluctuation-dissipation theorem [68,69], can fulfill Eq. (26). As shown also in the figure, the semilocal correlation functionals (e.g., PBE and PBEsol) fail badly at large wave vectors. In Fig. 8, we show the LDA, PBE, and YUKc correlation energy per particle  $\epsilon_c$  for the jellium cluster with 92  $e^-$  and  $r_s = 2$ , and the Ne atom, respectively. In both cases, the YUKc is close to and only slightly better than LDA. This is a consequence of the  $\beta^{\text{YUKc}}$  value. Finally, in Fig. 9 we show the correlation potential  $v_c = \delta E_c / \delta n$  for the Ne atom. While PBE, as any GGA and meta-GGA, diverges at the nucleus, the YUKc functional is finite but close to the LDA value. Overall, the  $v_c^{\text{YUKc}}$  improves over the  $v_c^{\text{LDA}}$ , but cannot describe the quantum oscillations.

#### IV. EXCHANGE-CORRELATION FUNCTIONALS FOR JELLIUM LINEAR RESPONSE

In this section we combine the YUKx exchange functionals with the YUKc correlation functional, showing the results for the HEG linear-response exchange-correlation function  $\gamma_{xc}$ . Thus, in Fig. 10, we report  $\gamma_{xc}$  of the uniform electron gases with  $r_s = 2$  and 5, respectively, for several functionals. PBE, which is based on a heavy error cancellation between its exchange and correlation parts, recovers (by construction) the accurate LDA linear response, being exact only at  $\eta = 0$ . On the other hand, PBEsol, which has been fitted to jellium surface XC energies, is moderately close to the CP and RA static kernels for  $\eta \leq 3$ , but at larger wave vectors is failing badly. Nevertheless, the best performance is provided by YUKx1+YUKc, which is very close to RA until  $\eta \leq 1$ . Note that in this region,  $\gamma_{xc}^{\text{RA}} \geq \gamma_{xc}^{\text{LDA}}$  and the same feature is also

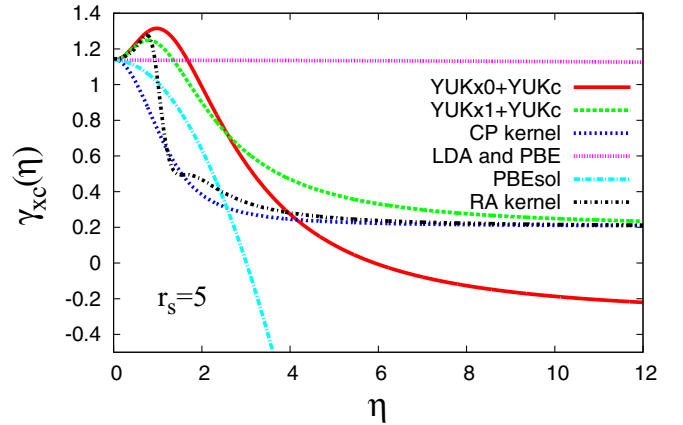
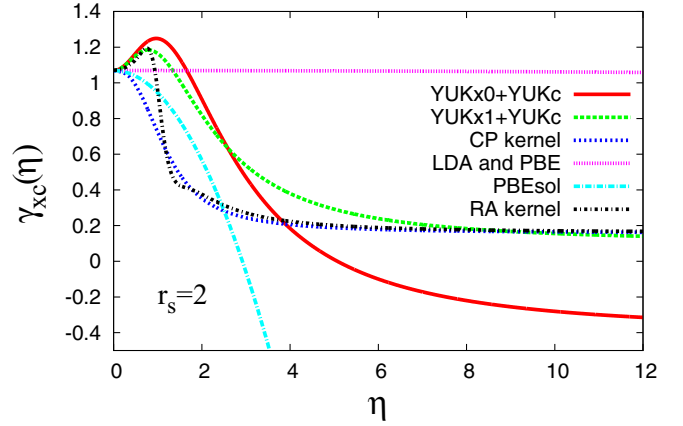


FIG. 10. The exchange-correlation linear response function  $\gamma_{xc}$  of the uniform electron gas, versus the dimensionless momentum  $\eta = k/2k_F$ , for  $r_s = 2$  and 5, respectively. We also show the results from the static ( $\omega = 0$ ) CP kernel of Ref. [72], and the static ( $\omega = 0$ ) state-of-the-art RA kernel of Ref. [77].

shown by other XC kernels [75,116], while the DMC data are quite noisy [98], and  $\gamma_{xc}^{\text{CP}} \leq \gamma_{xc}^{\text{LDA}}$  everywhere, recovering the compressibility sum rule at  $\eta = 0$ . For large wave vectors  $\eta \geq 4$ , YUKx1+YUKc is close to the exact behavior, which is incorporated in both CP and RA kernels.

Thus the YUKx1+YUKc functional provides also a physical pair distribution function at small interparticle distance, where semilocal functionals may fail badly [81,105]. On the other hand the YUKx1+YUKc functional, as well as jellium kernels in the linear response TDDFT, cannot describe excitonic effects of bulk semiconductors and insulators [73,117–119], yet its good behavior for  $\eta \rightarrow \infty$  may be still important for the electron energy loss spectra (EELS) at large momentum transfer [120].

We also recall that the jellium kernels in the linear response TDDFT approach perform accurately for the equilibrium lattice constants, bulk moduli, and correlation energies per electron of bulk solids [85]. However, these methods may not be suitable for double, Rydberg, and long-range charge transfer excitations [121], where additional corrections are required [122,123]. Nevertheless, the nonlocality of the YUKx1+YUKc functional can be important for the long-range charge-transfer excited states in TDDFT calculations [124].



## V. SUMMARY AND CONCLUSIONS

We have investigated the reduced, dimensionless Yukawa potential  $y_\alpha$  [see Eq. (1)] as an ingredient for the development of exchange and correlation functionals. First, we have constructed the YUKx0 and YUKx1 exchange functionals, having very simple exchange enhancement factors dependent only on  $y_\alpha$  [i.e.,  $F_x = F_x(y_\alpha)$ ]. Both YUKx0 and YUKx1 give HEG linear response exchange functions  $\gamma_x(\eta)$  that are correct at small wave vectors [recovering the second-order expansion  $\gamma_x(\eta) \rightarrow 1 + (5/9)\eta^2$ ], but also they are finite at large wave vectors, a feature that usually cannot be reached by semilocal exchange functionals. Moreover, the YUKx1 linear response exchange function  $\gamma_x(\eta)$  becomes even exact at large wave vectors.

We have also proposed the YUKx2 exchange functional, that preserves the YUKx1 linear response of the homogeneous electron gas, and becomes exact for any one- and two-electron systems. In this case, the YUKx2 exchange enhancement factor is dependent on both  $y_\alpha$  and  $z$  [i.e.,  $F_x = F_x(y_\alpha, z)$ ], where  $z$  is the well-known meta-GGA ingredient that can distinguish iso-orbital regions.

We tested the YUKx functionals for atoms and jellium clusters. Noting that these simple functionals have been constructed solely from the HEG linear response, their performances are very encouraging. In particular we have proved that they are close to exact at the nuclear cusp and in the inner atomic core, where both  $F_x$  and  $v_x$  are realistic. Such a feature can become important, showing that YUKx functionals are accurate for the short-range regime, and for example, they can be used in the construction of short-range screened functionals [103].

Next, we have developed the YUKc correlation functional, which is dependent only on the spin densities and  $y_\alpha$  [i.e.,  $\epsilon_c = \epsilon_c(n_\uparrow, n_\downarrow, y_\alpha)$ ]. The YUKc linear response function  $\gamma_c$  is moderately accurate for small and large wave vectors, which is an important achievement, met only by high-level, fifth-rung functionals. However, the performance of YUKc for atoms and jellium clusters is better than, but close to, the LDA. Thus, future work should be done to improve the YUKc for systems beyond the HEG linear response at small external perturbations.

Finally, the YUKx1+YUKc exchange-correlation functional gives a realistic HEG linear response function  $\gamma_{xc}$ , competing with the CP and RA kernels, as shown in Fig. 10. These results fully assess the  $y_\alpha$  as a powerful ingredient for the DFT development of the exchange-correlation functionals.

Moreover, the YUKx1+YUKc functional can be of interest for various applications in solid-state electronic calculations, and its nonlocality should be further investigated. However, the YUKx1+YUKc functional has been constructed only from a few exact conditions related mainly to the HEG linear response, and its accuracy for the total exchange-correlation energy is not as good as that of popular semilocal functionals. In order to improve it, one should consider incorporating other exact conditions relevant for the total exchange-correlation energy, such as the fourth-order gradient expansion of the exchange energy [92], the second-order gradient expansion of the correlation energy [94], and the semiclassical expansions of the neutral, nonrelativistic atoms for exchange [109–111] and correlation [125,126].

## APPENDIX A: COMPUTATIONAL DETAILS

All calculations are done non-self-consistently, using accurate numerical LDA orbitals and densities, in a modified version of the Engel code [2,127,128]. The KS-DFT LDA calculations have been performed with a logarithmic mesh with 800 points along the radial direction, in order to accurately capture the atomic nuclear cusp. The convergence criteria are as follows: (1) the difference between total energies of two consecutive iterations must be smaller than  $10^{-8}$  Ry, and (2) the maximum absolute difference between the total potentials of two consecutive iterations must be smaller than  $10^{-5}$ .

Neutral jellium clusters with  $Z$  electrons and radius  $R = r_s Z^{1/3}$  have the external potential [111]

$$v_{\text{ext}}^{\text{jell}}(r) = \begin{cases} Z(-\frac{3}{2R} + \frac{r^2}{2R^3}), & r < R, \\ -Z\frac{1}{r}, & r \geq R, \end{cases} \quad (\text{A1})$$

given by the positive background

$$n_+(\mathbf{r}) = \begin{cases} 3/4\pi r_s^3, & r < R, \\ 0, & r \geq R. \end{cases} \quad (\text{A2})$$

## APPENDIX B: DERIVATION OF THE LINEAR RESPONSE

We consider a small perturbation of the HEG, such that the perturbed density is  $n(\mathbf{r}) = n_0 + n_k e^{-i\mathbf{k}\mathbf{r}}$ , with  $n_0$  being the bulk density and  $n_k \ll n_0$ . Following the method described in Refs. [30,98,129], we replace the perturbed functional in the functional expression, taking the Taylor series in  $n_k/n_0$ . The linear response function  $\gamma_x$  of the considered functional will be the second-order coefficient of this expansion multiplied by  $-2k_F^2/\pi$ .

First, let us consider any Laplacian-level meta-GGA exchange functional with the enhancement factor  $F_x(s, q)$ , where  $s$  and  $q$  are the reduced gradient and Laplacian of the density. Note that our analysis can be applied to any meta-GGA functional, because the kinetic energy density  $\tau$  in the small- and large-wave-vector limits can be expressed in terms of  $n$ ,  $s$ , and  $q$  [98]. We assume that  $F_x(s, q)$  recovers the LDA behavior at  $s = q = 0$ , such that at small reduced gradients we have the general form

$$F_x(s, q) = 1 + a_1 s^2 + a_2 q + a_3 s^4 + a_4 q^2 + a_5 s^2 q + a_6 q^3 + a_7 s^6 + a_8 q s^4 + a_9 q^2 s^2 + \dots \quad (\text{B1})$$

Then, the linear response of this exchange functional is

$$\gamma_x^{\text{semilocal}} = 1 + \left(\frac{9}{2}a_1 + \frac{3}{2}a_2\right)\eta^2 + \frac{9}{2}a_4\eta^4. \quad (\text{B2})$$

Note that the terms  $s^2$  and  $q$  are interchangeable under integration by parts [108], and usually the  $q$  term is eliminated in favor of  $s^2$  term. Then, considering  $a_2 = 0$ ,  $a_1 = 10/81$ , and  $a_4 = 146/2025$  fixed from the gradient expansion of the exchange energy [92], we obtain

$$\gamma_x^{\text{semilocal}} = 1 + \frac{5}{9}\eta^2 + \frac{73}{225}\eta^4, \quad (\text{B3})$$

which is the exact behavior at small wave vectors. On the other hand,  $\gamma_x^{\text{semilocal}}$  is finite at large wave vectors, only if  $a_2 = -3a_1$  and  $a_4 = 0$ .

The linear response of the YUKx0 functional is computed using Eq. (G4) of Ref. [30],

$$\begin{aligned} \gamma_\alpha(\mathbf{r} = 0) = & 1 - \frac{k^2}{n_0[(3\pi^2)^{2/3}\alpha'^2 n_0^{2/3} + k^2]} n_k \\ & + \frac{1}{3n_0^2} \frac{k^2[5(3\pi^2)^{2/3}\alpha'^2 n_0^{2/3} + 3k^2]}{[(3\pi^2)^{2/3}\alpha'^2 n_0^{2/3} + k^2]^2} n_k^2 + O(n_k^3), \end{aligned} \quad (\text{B4})$$

where  $\alpha' = \alpha/\alpha_{k_F}$ . Multiplying Eq. (B4) with the LDA exchange energy density [computed at the density  $n(\mathbf{r} = 0) = n_0 + n_k$ ], we find, after some algebra, the expression of Eq. (6). Noting that the YUKx1 exchange functional is just a linear combination between LDA exchange and YUKx0, its linear response function can be easily computed, obtaining

$$\gamma_x^{\text{YUKx1}}(\eta) = \frac{\alpha^4 + (8 + 6\beta)\alpha^2 \alpha_{k_F}^2 \eta^2 - (24\beta - 16)\alpha_{k_F}^4 \eta^4}{(4\alpha_{k_F}^2 \eta^2 + \alpha^2)^2}. \quad (\text{B5})$$

When  $\beta = 1$ , Eq. (B5) recovers  $\gamma_x^{\text{YUKx0}}(\eta)$  of Eq. (6). When  $\beta = 0$ , Eq. (B5) recovers  $\gamma_x^{\text{LDA}}(\eta) = 1$ . Substituting  $\alpha$  and  $\beta$  of Eq. (11) into Eq. (B5), we obtain Eq. (12).

### APPENDIX C: OPTIMIZATION OF THE YUKx2 FUNCTIONAL

The parameter  $\alpha_2$  of Eq. (17) has been fitted to the exchange energies of noble atoms (from Ne to the nonrelativistic atom with 290  $e^-$ ), by minimizing the mean absolute relative error.

For a slowly varying density, the function  $c(z)$  behaves as

$$c(z) = (1 - z^3)^{1/6} \rightarrow 1 - z^3/6 + O(z^6), \quad (\text{C1})$$

such that the YUKx2 exchange enhancement factor is

$$F_x^{\text{YUKx2}} \approx \frac{z^3}{6} (\zeta_2 - F_x^{\text{YUKx1}}) + F_x^{\text{YUKx1}}. \quad (\text{C2})$$

Noting that  $z = \tau^W/\tau \approx (5s^2/3)$ , then the first term on the right-hand side of Eq. (C2) is a higher response term (see also Appendix B). Then, YUKx2 has the same linear response as the YUKx1 functional.

### APPENDIX D: OPTIMIZATION OF THE YUKc FUNCTIONAL

The HEG linear response of the YUKc correlation functional has been computed using the method described in Appendix B. However, because of the density dependence of  $\epsilon_c^{\text{LDA}}$  that enters into the YUKc expression, the final formula of  $\gamma_c$  is quite complicated. Then we find the parameters  $\alpha$  and  $\sigma$  by checking that the slope  $d\gamma_c/d\eta^2$  is negative at  $\eta = 0$ , and minimizing the errors between the computed  $\gamma_c$  and Eq. (26) at large wave vectors, in the physically motivated range  $2 \leq r_s \leq 6$  for bulk metals.

Now, let us consider the high-density (HD) and low-density (LD) limits. For the HD case, we consider  $\epsilon_c^{\text{LDA}} \approx c_0(\zeta) \ln(r_s)$  [91]; then we obtain

$$\begin{aligned} \gamma_c^{\text{HD}} \rightarrow & \frac{c_0 r_s 2^{2/3} \pi^{2/3} \sqrt[3]{3}}{3} \\ & + 8 \frac{\pi^2 [2 \ln(r_s) + 1] 2^{2/3} r_s c_0}{(1 + \sigma) \alpha^2} \eta^2 \\ & + O(\eta^4), \quad \text{when } \eta \rightarrow 0, \\ \gamma_c^{\text{HD}} \rightarrow & - \frac{c_0 r_s 2^{2/3} \pi^{2/3} \sqrt[3]{3} [-\sigma^2 + 6 \ln(r_s) - 4\sigma - 3]}{3(\sigma^2 + 2\sigma + 1)}, \\ & \text{when } \eta \rightarrow \infty. \end{aligned} \quad (\text{D1})$$

On the other hand, in the LD case, the first-order term of the LDA correlation scales as exchange, such that  $\epsilon_c^{\text{LDA}} \approx -d_0(\zeta)/r_s$  [91]; then  $\gamma_c^{\text{LD}}$  has a simpler expression, being independent of  $r_s$ :

$$\begin{aligned} \gamma_c^{\text{LD}} = & \frac{4}{9} [\sqrt[3]{3} \pi^{2/3} 2^{2/3} d_0 (\alpha^4 + 2 \cdot 3^{2/3} \pi^{4/3} \alpha^2 \eta^2 \\ & + 336 \sqrt[3]{3} \pi^{8/3} \eta^4 + 48 \sqrt[3]{3} \pi^{8/3} \eta^4 \sigma^2 \\ & + 8 \sigma^2 3^{2/3} \pi^{4/3} \alpha^2 \eta^2 \\ & + \alpha^4 \sigma^2 + 2 \alpha^4 \sigma + 10 \sigma 3^{2/3} \pi^{4/3} \alpha^2 \eta^2 \\ & + 168 \sqrt[3]{3} \pi^{8/3} \eta^4 \sigma)] / [(\sigma^2 + 2\sigma + 1) \\ & \times (4 \cdot 3^{2/3} \pi^{4/3} \eta^2 + \alpha^2)^2], \end{aligned} \quad (\text{D2})$$

which behaves as

$$\begin{aligned} \gamma_c^{\text{LD}} \rightarrow & \frac{4 d_0 2^{2/3} \pi^{2/3} \sqrt[3]{3}}{9} - \frac{8 \pi^2 2^{2/3} d_0}{(1 + \sigma) \alpha^2} \eta^2 + \dots \quad \text{when } \eta \rightarrow 0, \\ \gamma_c^{\text{LD}} \rightarrow & \frac{2 d_0 2^{2/3} \pi^{2/3} \sqrt[3]{3} (2\sigma^2 + 7\sigma + 14)}{9(\sigma^2 + 2\sigma + 1)}, \quad \text{when } \eta \rightarrow \infty. \end{aligned} \quad (\text{D3})$$

We observe that both  $\gamma_c^{\text{HD}}$  and  $\gamma_c^{\text{LD}}$  have negative slopes ( $d\gamma_c/d\eta^2 \leq 0$ ), and both are positive at large wave vectors.

- [1] W. Kohn and L. J. Sham, *Phys. Rev.* **140**, A1133 (1965).
- [2] E. Engel and R. M. Dreizler, *Density Functional Theory* (Springer, Berlin, Heidelberg, 2013).
- [3] J. F. Dobson, G. Vignale, and M. P. Das, *Electronic Density Functional Theory* (Springer, Oxford, 1998).
- [4] R. G. Parr and W. Yang, *Density-Functional Theory of Atoms and Molecules* (Oxford University Press, New York, 1989).

- [5] *Recent Developments and Applications of Modern Density Functional Theory*, edited by J. M. Seminario (Elsevier, New York, 1996).
- [6] D. Sholl and J. A. Steckel, *Density Functional Theory: A Practical Introduction* (Wiley, New Jersey, 2009).
- [7] R. O. Jones, *Rev. Mod. Phys.* **87**, 897 (2015).
- [8] E. J. Baerends, *Phys. Rev. Lett.* **87**, 133004 (2001).

- [9] B. Kanungo, P. M. Zimmerman, and V. Gavini, *Nat. Commun.* **10**, 1 (2019).
- [10] K. Burke, *J. Chem. Phys.* **136**, 150901 (2012).
- [11] R. Peverati and D. G. Truhlar, *Philos. Trans. R. Soc. A* **372**, 20120476 (2014).
- [12] A. D. Becke, *J. Chem. Phys.* **140**, 18A301 (2014).
- [13] M. Levy, *Int. J. Quantum Chem.* **116**, 802 (2016).
- [14] G. E. Scuseria and V. N. Staroverov, in *Theory and Applications of Computational Chemistry* (Elsevier, Amsterdam, 2005), pp. 669–724.
- [15] F. Della Sala, E. Fabiano, and L. A. Constantin, *Int. J. Quantum Chem.* **116**, 1641 (2016).
- [16] J. P. Perdew and K. Schmidt, *AIP Conf. Proc.* **577**, 1 (2001).
- [17] S. Śmiga and L. A. Constantin, *J. Phys. Chem. A* **124**, 5606 (2020).
- [18] B. G. Janesko and A. Agüero, *J. Chem. Phys.* **136**, 024111 (2012).
- [19] B. G. Janesko, *Int. J. Quantum Chem.* **113**, 83 (2013).
- [20] B. G. Janesko, *J. Chem. Phys.* **133**, 104103 (2010).
- [21] B. G. Janesko, *J. Chem. Phys.* **137**, 224110 (2012).
- [22] B. G. Janesko, E. Proynov, G. Scalmani, and M. J. Frisch, *J. Chem. Phys.* **148**, 104112 (2018).
- [23] O. Gunnarsson, M. Jonson, and B. Lundqvist, *Solid State Commun.* **24**, 765 (1977).
- [24] J. A. Alonso and L. A. Girifalco, *Phys. Rev. B* **17**, 3735 (1978).
- [25] Z. Wu, R. E. Cohen, and D. J. Singh, *Phys. Rev. B* **70**, 104112 (2004).
- [26] D. J. Singh, *Phys. Rev. B* **48**, 14099 (1993).
- [27] O. Gunnarsson, M. Jonson, and B. I. Lundqvist, *Phys. Rev. B* **20**, 3136 (1979).
- [28] L. A. Constantin, E. Fabiano, and F. Della Sala, *J. Chem. Phys.* **145**, 084110 (2016).
- [29] L. A. Constantin, E. Fabiano, and F. Della Sala, *J. Chem. Theory Comput.* **13**, 4228 (2017).
- [30] F. Sarcinella, E. Fabiano, L. A. Constantin, and F. Della Sala, *Phys. Rev. B* **103**, 155127 (2021).
- [31] J. P. Perdew, V. N. Staroverov, J. Tao, and G. E. Scuseria, *Phys. Rev. A* **78**, 052513 (2008).
- [32] J. P. Perdew, A. Ruzsinszky, J. Tao, V. N. Staroverov, G. E. Scuseria, and G. I. Csonka, *J. Chem. Phys.* **123**, 062201 (2005).
- [33] M. M. Odashima and K. Capelle, *Phys. Rev. A* **79**, 062515 (2009).
- [34] A. V. Arbuznikov and M. Kaupp, *Int. J. Quantum Chem.* **111**, 2625 (2011).
- [35] J. Jaramillo, G. E. Scuseria, and M. Ernzerhof, *J. Chem. Phys.* **118**, 1068 (2003).
- [36] S. Kümmel and L. Kronik, *Rev. Mod. Phys.* **80**, 3 (2008).
- [37] A. D. Becke, *J. Chem. Phys.* **122**, 064101 (2005).
- [38] A. D. Becke and E. R. Johnson, *J. Chem. Phys.* **127**, 124108 (2007).
- [39] A. D. Becke, *J. Chem. Phys.* **119**, 2972 (2003).
- [40] A. D. Becke, *J. Chem. Phys.* **138**, 074109 (2013).
- [41] E. Fabiano, L. A. Constantin, and F. Della Sala, *Int. J. Quantum Chem.* **113**, 673 (2013).
- [42] E. Fabiano, L. A. Constantin, P. Cortona, and F. Della Sala, *J. Chem. Theory Comput.* **11**, 122 (2014).
- [43] R. J. Bartlett, I. Grabowski, S. Hirata, and S. Ivanov, *J. Chem. Phys.* **122**, 034104 (2005).
- [44] R. J. Bartlett, V. F. Lotrich, and I. V. Schweigert, *J. Chem. Phys.* **123**, 062205 (2005).
- [45] I. Grabowski, E. Fabiano, and F. Della Sala, *Phys. Rev. B* **87**, 075103 (2013).
- [46] I. Grabowski, E. Fabiano, A. M. Teale, S. Śmiga, A. Buksztel, and F. Della Sala, *J. Chem. Phys.* **141**, 024113 (2014).
- [47] S. Jana, S. Śmiga, L. A. Constantin, and P. Samal, *J. Chem. Theory Comput.* **16**, 7413 (2020).
- [48] M. Seidl, J. P. Perdew, and S. Kurth, *Phys. Rev. Lett.* **84**, 5070 (2000).
- [49] M. Seidl, J. P. Perdew, and S. Kurth, *Phys. Rev. A* **62**, 012502 (2000).
- [50] J. P. Perdew, S. Kurth, and M. Seidl, *Int. J. Mod. Phys. B* **15**, 1672 (2001).
- [51] Z.-F. Liu and K. Burke, *Phys. Rev. A* **79**, 064503 (2009).
- [52] Z.-F. Liu and K. Burke, *J. Chem. Phys.* **131**, 124124 (2009).
- [53] R. Magyar, W. Terilla, and K. Burke, *J. Chem. Phys.* **119**, 696 (2003).
- [54] J. Sun, *J. Chem. Theory Comput.* **5**, 708 (2009).
- [55] M. Seidl and P. Gori-Giorgi, *Phys. Rev. A* **81**, 012508 (2010).
- [56] P. Gori-Giorgi, G. Vignale, and M. Seidl, *J. Chem. Theory Comput.* **5**, 743 (2009).
- [57] A. Mirschink, M. Seidl, and P. Gori-Giorgi, *J. Chem. Theory Comput.* **8**, 3097 (2012).
- [58] P. Gori-Giorgi and M. Seidl, *Phys. Chem. Chem. Phys.* **12**, 14405 (2010).
- [59] S. Vuckovic, T. J. Irons, A. Savin, A. M. Teale, and P. Gori-Giorgi, *J. Chem. Theory Comput.* **12**, 2598 (2016).
- [60] E. Fabiano, P. Gori-Giorgi, M. Seidl, and F. Della Sala, *J. Chem. Theory Comput.* **12**, 4885 (2016).
- [61] S. Giarrusso, P. Gori-Giorgi, F. Della Sala, and E. Fabiano, *J. Chem. Phys.* **148**, 134106 (2018).
- [62] E. Fabiano, S. Śmiga, S. Giarrusso, T. J. Daas, F. Della Sala, I. Grabowski, and P. Gori-Giorgi, *J. Chem. Theory Comput.* **15**, 1006 (2019).
- [63] S. Vuckovic, P. Gori-Giorgi, F. Della Sala, and E. Fabiano, *J. Phys. Chem. Lett.* **9**, 3137 (2018).
- [64] D. P. Kooi and P. Gori-Giorgi, *Theor. Chem. Acc.* **137**, 166 (2018).
- [65] Y. Zhou, H. Bahmann, and M. Ernzerhof, *J. Chem. Phys.* **143**, 124103 (2015).
- [66] L. A. Constantin, *Phys. Rev. B* **99**, 085117 (2019).
- [67] S. Śmiga and L. A. Constantin, *J. Chem. Theory Comput.* **16**, 4983 (2020).
- [68] J. Harris and A. Griffin, *Phys. Rev. B* **11**, 3669 (1975).
- [69] D. C. Langreth and J. P. Perdew, *Phys. Rev. B* **15**, 2884 (1977).
- [70] J. Toulouse, I. C. Gerber, G. Jansen, A. Savin, and J. G. Ángyán, *Phys. Rev. Lett.* **102**, 096404 (2009).
- [71] J. F. Dobson, J. Wang, and T. Gould, *Phys. Rev. B* **66**, 081108(R) (2002).
- [72] L. A. Constantin and J. M. Pitarke, *Phys. Rev. B* **75**, 245127 (2007).
- [73] A. V. Terentjev, L. A. Constantin, and J. M. Pitarke, *Phys. Rev. B* **98**, 085123 (2018).
- [74] L. A. Constantin, *Phys. Rev. B* **93**, 121104(R) (2016).
- [75] M. Corradini, R. Del Sole, G. Onida, and M. Palumbo, *Phys. Rev. B* **57**, 14569 (1998).
- [76] J. Toulouse, *Phys. Rev. B* **72**, 035117 (2005).
- [77] C. F. Richardson and N. W. Ashcroft, *Phys. Rev. B* **50**, 8170 (1994).

- [78] J. E. Bates, S. Laricchia, and A. Ruzsinszky, *Phys. Rev. B* **93**, 045119 (2016).
- [79] J. E. Bates, J. Sensenig, and A. Ruzsinszky, *Phys. Rev. B* **95**, 195158 (2017).
- [80] A. Ruzsinszky, L. A. Constantin, and J. M. Pitarke, *Phys. Rev. B* **94**, 165155 (2016).
- [81] J. F. Dobson and J. Wang, *Phys. Rev. B* **62**, 10038 (2000).
- [82] A. Görling, *Int. J. Quantum Chem.* **69**, 265 (1998).
- [83] Y.-H. Kim and A. Görling, *Phys. Rev. Lett.* **89**, 096402 (2002).
- [84] J. Erhard, P. Bleiziffer, and A. Görling, *Phys. Rev. Lett.* **117**, 143002 (2016).
- [85] C. E. Patrick and K. S. Thygesen, *J. Chem. Phys.* **143**, 102802 (2015).
- [86] A. Ruzsinszky, N. K. Nepal, J. M. Pitarke, and J. P. Perdew, *Phys. Rev. B* **101**, 245135 (2020).
- [87] N. K. Nepal, A. D. Kaplan, J. M. Pitarke, and A. Ruzsinszky, *Phys. Rev. B* **104**, 125112 (2021).
- [88] J. Sun, A. Ruzsinszky, and J. P. Perdew, *Phys. Rev. Lett.* **115**, 036402 (2015).
- [89] M. Levy and J. P. Perdew, *Int. J. Quantum Chem.* **49**, 539 (1994).
- [90] S. Moroni, D. M. Ceperley, and G. Senatore, *Phys. Rev. Lett.* **75**, 689 (1995).
- [91] J. P. Perdew and Y. Wang, *Phys. Rev. B* **45**, 13244 (1992).
- [92] P.-S. Svendsen and U. von Barth, *Phys. Rev. B* **54**, 17402 (1996).
- [93] P. R. Antoniewicz and L. Kleinman, *Phys. Rev. B* **31**, 6779 (1985).
- [94] C. D. Hu and D. C. Langreth, *Phys. Rev. B* **33**, 943 (1986).
- [95] S.-K. Ma and K. A. Brueckner, *Phys. Rev.* **165**, 18 (1968).
- [96] P.-S. Svendsen and U. Von Barth, *Int. J. Quantum Chem.* **56**, 351 (1995).
- [97] E. Engel and S. H. Vosko, *Phys. Rev. B* **50**, 10498 (1994).
- [98] J. Tao, J. P. Perdew, L. M. Almeida, C. Fiolhais, and S. Kümmel, *Phys. Rev. B* **77**, 245107 (2008).
- [99] J. P. Perdew, K. Burke, and M. Ernzerhof, *Phys. Rev. Lett.* **77**, 3865 (1996).
- [100] L. A. Constantin, E. Fabiano, S. Laricchia, and F. Della Sala, *Phys. Rev. Lett.* **106**, 186406 (2011).
- [101] L. A. Constantin, A. Terentjevs, F. Della Sala, P. Cortona, and E. Fabiano, *Phys. Rev. B* **93**, 045126 (2016).
- [102] S. Jana, A. Patra, L. A. Constantin, H. Myneni, and P. Samal, *Phys. Rev. A* **99**, 042515 (2019).
- [103] S. Jana, A. Patra, L. A. Constantin, and P. Samal, *J. Chem. Phys.* **152**, 044111 (2020).
- [104] S. Jana, B. Patra, S. Śmiga, L. A. Constantin, and P. Samal, *Phys. Rev. B* **102**, 155107 (2020).
- [105] F. Furche and T. Van Voorhis, *J. Chem. Phys.* **122**, 164106 (2005).
- [106] J. P. Perdew, A. Ruzsinszky, G. I. Csonka, O. A. Vydrov, G. E. Scuseria, L. A. Constantin, X. Zhou, and K. Burke, *Phys. Rev. Lett.* **100**, 136406 (2008).
- [107] J. Tao, V. N. Staroverov, G. E. Scuseria, and J. P. Perdew, *Phys. Rev. A* **77**, 012509 (2008).
- [108] A. C. Cancio, C. E. Wagner, and S. A. Wood, *Int. J. Quantum Chem.* **112**, 3796 (2012).
- [109] P. Elliott, D. Lee, A. Cangì, and K. Burke, *Phys. Rev. Lett.* **100**, 256406 (2008).
- [110] P. Elliott and K. Burke, *Can. J. Chem.* **87**, 1485 (2009).
- [111] E. Fabiano and L. A. Constantin, *Phys. Rev. A* **87**, 012511 (2013).
- [112] H. M. Baghramyan, F. Della Sala, and C. Ciraci, *Phys. Rev. X* **11**, 011049 (2021).
- [113] M. Brack, *Rev. Mod. Phys.* **65**, 677 (1993).
- [114] J. P. Perdew, A. Ruzsinszky, G. I. Csonka, L. A. Constantin, and J. Sun, *Phys. Rev. Lett.* **103**, 026403 (2009).
- [115] T. Chachiyo, *J. Chem. Phys.* **145**, 021101 (2016).
- [116] S. Ichimaru and K. Utsumi, *Phys. Rev. B* **24**, 7385 (1981).
- [117] P. E. Trevisanutto, A. Terentjevs, L. A. Constantin, V. Olevano, and F. Della Sala, *Phys. Rev. B* **87**, 205143 (2013).
- [118] Y.-M. Byun, J. Sun, and C. A. Ullrich, *Electron. Struct.* **2**, 023002 (2020).
- [119] Y.-M. Byun and C. A. Ullrich, *Phys. Rev. B* **95**, 205136 (2017).
- [120] S. Sharma, J. Dewhurst, A. Sanna, A. Rubio, and E. Gross, *New J. Phys.* **14**, 053052 (2012).
- [121] Y. Yang, H. van Aggelen, and W. Yang, *J. Chem. Phys.* **139**, 224105 (2013).
- [122] J. Neugebauer, O. Gritsenko, and E. J. Baerends, *J. Chem. Phys.* **124**, 214102 (2006).
- [123] N. T. Maitra, *J. Phys.: Condens. Matter* **29**, 423001 (2017).
- [124] A. Dreuw, J. L. Weisman, and M. Head-Gordon, *J. Chem. Phys.* **119**, 2943 (2003).
- [125] K. Burke, A. Cancio, T. Gould, and S. Pittalis, *J. Chem. Phys.* **145**, 054112 (2016).
- [126] A. Cancio, G. P. Chen, B. T. Krull, and K. Burke, *J. Chem. Phys.* **149**, 084116 (2018).
- [127] E. Engel and S. H. Vosko, *Phys. Rev. A* **47**, 2800 (1993).
- [128] E. Engel, in *A Primer in Density Functional Theory* (Springer, Berlin, Heidelberg, 2003), pp. 56–122.
- [129] L. A. Constantin, E. Fabiano, S. Śmiga, and F. Della Sala, *Phys. Rev. B* **95**, 115153 (2017).